

Heterogeneous recovery guided by policies from large scale power failures

Amir Hossein Afsharinejad¹, Chuanyi Ji¹ and Robert Wilcox²

¹*School of Electrical and Computer Engineering, Georgia Institute of Technology, Atlanta, Georgia 30332–0250*

²*National Grid, Waltham, Massachusetts 02451*

³*Corresponding author: Chuanyi Ji, School of Electrical and Computer Engineering, Georgia Institute of Technology, Atlanta, Georgia 30332–0250, Tel:404-894-2393, jichuanyi@gatech.edu*

Abstract

Large-scale power failures are induced by nearly all natural disasters from hurricanes to wild fires. A fundamental problem is whether and how recovery guided by government policies is able to meet the challenge of a wide range of disruptions. Prior research on this problem is scant due to lack of sharing large-scale granular data at the operational energy grid, stigma of revealing limitations of services, and complex recovery coupled with policies and customers. As such, both quantification and firsthand information are lacking on capabilities and fundamental limitation of energy services in response to extreme events. Furthermore, government policies that guide recovery are often sidelined by prior study. This work studies the fundamental problem through the lens of recovery guided by two commonly adopted policies. We develop data analysis on unsupervised learning from non-stationary data. The data span failure events, from moderate to

extreme, at the operational distribution grid during the past nine years in two service regions at the state of New York and Massachusetts. We show that under the prioritization policy favoring large failures, recovery exhibits a surprising scaling property which counteracts failure scaling on the infrastructure vulnerability. However, heterogeneous recovery widens with the severity of failure events: large failures that cannot be prioritized increase customer interruption time by 47 folds. And, prolonged small failures dominate the entire temporal evolution of recovery.

Key words: Recovery guided by policies, power failures, granular data at scale, data analytics

Introduction

Natural disasters happen with increasing intensity in the US and the world ^{1,2}. Recovery from disruptions is thus crucial for sustaining our society. In this context, a fundamental problem is whether and how recovery responses guided by government policies is able to meet the challenge of a wide range of disruptions from the moderate to severe and extreme. This problem, while relevant to most infrastructures supporting our society, is particularly acute to the energy grid. Indeed, large-scale power failures were induced by nearly all natural disasters from hurricanes to severe ice storms and wild fire ^{1,3,4}. Millions of people lost electricity supplies for extended durations ^{1,3}. As such, this work studies the fundamental problem through the lens of recovery from large scale power failures.

Recovery from large-scale power failures exhibits a typical setting that involves service providers, customers, and government policies which guide the restoration ^{1,5,6}. The complexity

of such an interconnection hampers the study of recovery tremendously. A large volume of work develops algorithms for expediting recovery (see publications ^{7,8} and references therein). However, field studies on recovery services, i.e., using data from the operational grid and customers, are particularly lacking across a wide range of failure events from the moderate to extreme. As a result, there does not exist an established benchmark measuring the performance of recovery guided by underlying policies ⁹. In particular, knowledge is much needed on (a) how the recovery services perform across failure events of different intensity in the first place, and (b) capabilities and fundamental limitations of recovery guided by well adopted policies seen by the field data.

A key challenge for such a field study originates from the lack of granular data at a large scale. This has taken two forms: a singular focus on individual extreme events, and spatial temporal aggregation. First, failure event data are unevenly adopted across a range of severity; the failure events that have been studied are usually those severe enough to make the headline news ¹⁰. These events are often studied individually, including our own prior work ¹¹⁻¹³. Using individual failure events, however, does not allow a systematic study on whether recovery service can sustain desirable performance from failure events of increasing severity. Second, most work on historic power failures and recovery has used data aggregated over townships and hours since the granular measurements are privately owned and thus difficult to obtain ^{11,14}. Advanced data collection and analysis are emerging from smart meter infrastructure and micro PMUs ^{15,16}. Unfortunately, such advanced data collection is not widely deployed due to high costs.

This work conducts a large-scale field study of such nature that evaluates recovery services

from power failures. Specifically, we focus on recovery services that tie closely with a well adopted by emergency responders in general, i.e., to help as many people as fast as possible under resource constraints ^{1,17}. Distribution grid operators implement this guiding principle as they triage, i.e., to prioritize restoration of the large failures that affect a high number of customers ^{17,18}. There have been contentious opinions on the services guided by such recovery policy: (a) adopted by providers and disaster responders as a gold standard ¹⁷, but often complained by customers for slow recovery from disruptions ¹, and (b) potential weaknesses demonstrated by a few recent works on algorithm design ⁷ and case study ^{11,19}. There has not been a related systematic study across a wide range of failure events of different intensity. The policy itself has been largely sidelined by the prior work.

We take a data science approach for the field study. First, we collect large-scale data on recovery from power failures over the years 2011-2019 at the two service regions in the state of New York and Massachusetts. The data are commonly available to, but privately owned by, most of the distribution grid operators in the US and parts of the world ^{9,11}. The data are granular in geo-location and time, making it possible to relate restoration of the grid to impacted customers at the micro-level ^{9,11}. Second, we develop a mathematical framework to formulate recovery study through unsupervised learning ^{21,22}, an AI approach that is widely used in many application domains but yet to show wide potential in the energy area. The analytics algorithm learns from the non-stationary behaviors of recovery over the failure events of different severity. The data analysis brings new knowledge, centered around heterogeneous recovery in three aspects.

First, the recovery behaviors are found to be heterogeneous. That is, the failures that af-

fect large and small number of people recover at a disproportional share of customer interruption time. The large failures, in particular, affected clusters of customers but were restored with priority for helping the majority of the users. Surprisingly, such disparate recovery counteracts the infrastructure vulnerability found in the prior work ¹¹, showing the capability of services guided by prioritization policy.

Second, the disparity, as a generic characteristic of the prioritized recovery, deepens with the increasing severity of failure events. The discrepancy lies in both large and small failures: a significant increase of the large failures that cannot be prioritized, and domination of small failures throughout the dynamic evolution of delayed recovery. These findings tell us that the services governed by the prioritized recovery policy is at the cost of the disparity from both large and small failures; and the cost is significant when failure events become severe and extreme.

Results

Ensemble of failure events

We collect the granular data on failure and recovery at the service territories in the two US states during 2011-2019 (see Supplemental Tables 2 and 5). The first data set is obtained from 25,013 square miles in the state of New York. This data set is used in our primary study of the services guided by the recovery policy. The second data set consists of failure events at the state of Massachusetts over the same time span (see Supplemental Note 6, Supplemental Tables 4 and 5 for details). The data set from Massachusetts is intended for generalizing our study to a different state.

The primary data set consists of 53,070 failures from 172 events of different severity that affected over 9.7 million customers. In particular, 60 such failure events were induced by the so-called major storms declared by the state of New York (see Materials and methods and Supplemental Note 1). Six such failure events are further considered as extreme based on the total number of induced failures and the longest downtime duration of ~ 170 hours. For example, Hurricane Irene 2011 and Nor'easters 2018 are two of the named major storms that caused widespread disruptions. The other 54 failure events that were also caused by major storms are not as extreme and thus referred to as severe failure events. We identify additional 112 moderate failure events during the same time span. These moderate failures events were not induced by the declared major storms but impacted the grid more than sporadic failures in normal daily operations (Supplemental Note 1). Such moderate failure events were considered as unimportant, and thus have not been included in the prior studies. Together, our data are on the three types of failure events: the moderate, severe and extreme; three types define the severity of failure events. The failure events are induced by a wide range of weather conditions (see Materials and methods). For example, the six extreme failure events were induced by three severe thunderstorms, a hurricane, and two ice storms²³.

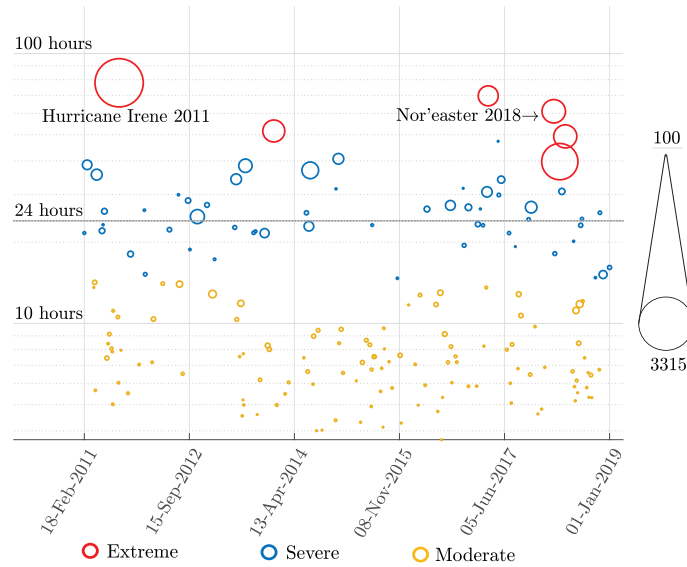
An overview in Fig. 1a shows the ensemble of failure events of all severities. An individual event has 101 \sim 519, 106 \sim 1146 and 1373 \sim 3315 total failures for the moderate, severe and extreme disruptions, respectively. The recovery services were able to restore electricity service within 24 hours for every moderate failure event. The downtime duration exceeded 24 hours per (major) event remained steady for the severe disruptions. The service deteriorated in the extreme failure events, with the downtime up to seven days. Hence, these three groups of disruptions

characterize a wide range of failure events of different severity.

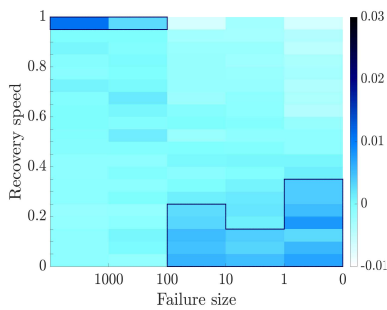
Distinct categories on recovery speed and failure size

We derive a mathematical framework that formulates our study as evaluation of recovery services based on unsupervised learning from the non-stationary data (see Materials and methods). Two covariates emerge as pertinent among the multiple variables relating to our data: (a) the recovery speed as the downtime duration ranked from the shortest to the longest; and (b) the failure size as the number of customers affected by a failure. These two variables together reflect the impact of the recovery policy (i.e., the utility triage) that prioritizes restoration of failures with a high number of affected customers¹⁷. The unsupervised learning algorithm then obtains the clustered regions in Figures 1b, 1c and 1d, where the recovery speed and failure size are positively dependent (see Materials and methods, and Supplemental Note 2). These clusters partition the space spanned by the recovery speed and failure size into the following four categories for all three types of events:

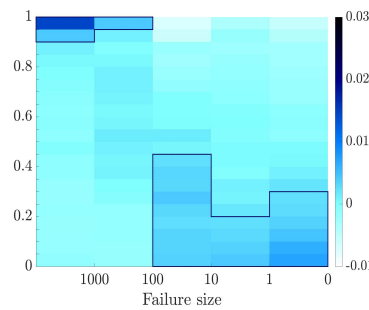
- **Prioritized large failures:** Each large failure affected more than 100 customers, and, the recovery speed is ranked within the top 15% shortest downtime durations. Such a fast recovery speed is strongly dependent of the large failure size, showing that the large failures are often restored with priority and rapidly.
- **Non-prioritized large failures:** Each failure has the same large size of affecting more than 100 customers. The recovery speed, however, is below the top 15% and nearly independent of the failure size.



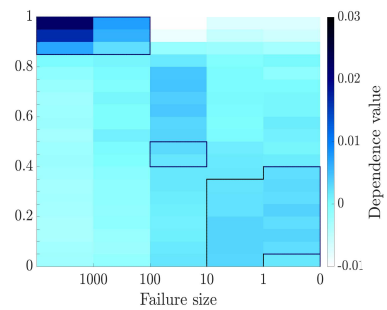
(a) Overview of failure events



(b) Extreme



(c) Severe



(d) Moderate

Figure 1: (a) Overview of failure events: 172 failure events from the moderate to severe and extreme, February 2011 to January 2019. Horizontal axis shows an event occurrence time. Vertical axis is on (the longest) recovery durations in logarithmic scale, where 95% of the failures recovered for each event. The radius of a marker represents the number of failures of a disruptive event from 100 to 3315 failures in Hurricane Irene. Red, blue and yellow markers correspond to extreme, severe and moderate events, respectively. (b), (c) and (d): Four categories of recovery speed and failure size. Statistical dependence between the recovery speed and failure size is averaged over the failure events for (b) extreme, (c) severe and (d) moderate disruptions respectively. Horizontal axis shows the failure size and vertical axis represents the recovery speed from 1 (the fastest) to 0 (the slowest). Color bar shows the values of statistical dependence. The boundaries highlight the two regions: (i) Prioritized large failures with rapid recovery at the upper left and (ii) Prolonged small failures with slow recovery at the lower right. The average value of statistical dependence within the boundaries exceeds 5% of the maximum value.

- Prolonged small failures: Each failure affected fewer than 100 customers, and, the recovery speed is ranked at within the bottom 50 ~ 100% of the longest failure durations. The slow recovery speed is strongly dependent of the small failure size, showing that those small failures experienced relatively long downtime durations.
- Remaining small failures: Each failure has the same small size of affecting fewer than 100 customers, and, the recovery speed is ranked higher than the percentage defined by the bottom cluster. The recovery speed is nearly independent of the failure size.

Here, we find that two clustered regions stand out in Figures 1b, 1c and 1d. The first is on the recovery of the prioritized large failures, where the dependence shown by the cluster implies that the large failures are potentially restored with priority soon after experiencing outages. The second is on the recovery of the prolonged small failures, where the long downtime durations are highly dependent of the small failure size, suggesting that the small failures often suffer delays in restoration. Despite the differences in the detailed shapes, these disparate clusters persist from the moderate to severe and extreme failure events.

Heterogeneous restoration behavior characterized by recovery scaling law

We define a recovery scaling law to quantify the different restoration behaviors from the four categories. While the failure scaling laws of different forms exist^{11,24}, recovery scaling does not. The recovery scaling law we define is a mapping between two quantities. The first is the probability $P_r(d)$ that a failure is restored within the top $d\%$ fastest (ranked by the failure durations from short-

est to longest). The second is the probability $P_c(x)$ that a customer is affected by such a failure which disrupts the service of more than x users (i.e., x is the failure size). Such a recovery scaling law essentially characterizes relationships between the percentage of customers recovered and cost as the share of interruption durations. The corresponding empirical probability distributions $\tilde{P}_r(d)$ and $\tilde{P}_c(x)$ estimate the scaling property using the data from the inferred clusters (Supplemental Note 3). The resulting empirical recovery scaling law is shown in Fig. 2 for three types of disruptive events from the moderate to severe and extreme (Supplemental Note 3).

The heterogeneous behavior emerges from the recovery scaling law as a prominent attribute. The recovery scaling follows the generalized 90-10 rule, where 92% \sim 94% affected customers consume 8% \sim 14% of the total interruption time. Importantly, these \sim 90% customers are affected by the large failures. Meanwhile, the prolonged small failures, while only amounting to less than 10% of the affected customers, consume 85% \sim 88% of the total interruption durations. Such disproportionality is present across the moderate, severe and extreme events as shown by the recovery scaling curves of the similar shapes. Phenomenologically, the disparate recovery between the large and small failures is consistent to the typical restoration guided by the recovery policy. The resulting restoration behaviors are bound to be heterogeneous if the recovery policy prioritizes large failures.

Interestingly, we discover that the recovery scaling mirrors the failure scaling when we extend the failure scaling law in our prior work¹¹ using the historic data. The failure scaling obeys a generalized 25-90 rule in Fig. 2 (20-80 in layman's terms). A small fraction (top 25%) of the large

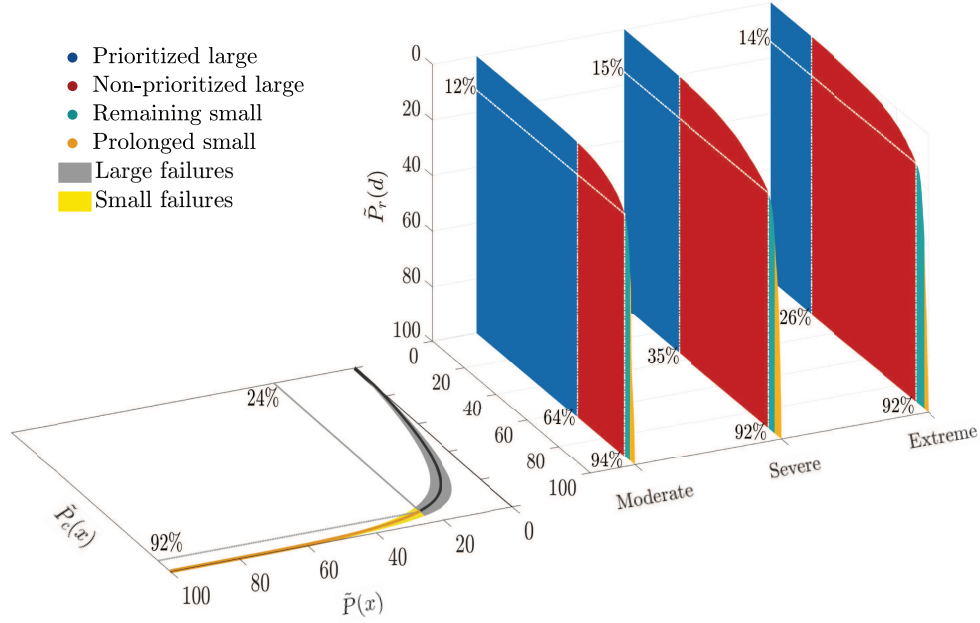


Figure 2: Right: Recovery scaling law for the moderate, severe and extreme failure events. $\tilde{P}_c(x)$: the empirical probability as the cumulative percentage of affected customers. $\tilde{P}_r(d)$: the empirical probability $\tilde{P}_r(d)$ as the cumulative percentage of the interruption durations. These probabilities are estimated for the four inference regions: The blue, red, green and yellow colors correspond to prioritized-large, non-prioritized-large, remaining-small and prolonged-small failures, respectively. Left: Failure scaling law. The vertical axis on $\tilde{P}_c(x)$ is the same as recovery scaling, and $\tilde{P}(x)$ is the empirical probability that a disruption affected more than x customers. The failure scaling curve is averaged over all failure events. The shaded regions illustrate standard deviation of the average. The grey and yellow colors are for large (more than 100 affected customers) and small (fewer than 100 impacted users) failures, respectively.

failures is responsible for the majority ($\sim 92\%$) of the affected customers. Basically, a large failure affected a block of customers, which is an infrastructural vulnerability of the distribution grid ¹¹. The restoration prioritized the large failures so that the blocks of customers recovered in relatively short downtime durations. In comparison, the prolonged small failures amount to a larger portion ($\sim 37\%$) of all failures but affected less than 10% customers. Hence, the data analysis helps connect the two scaling laws in a loop, making us to realize that the recovery services governed by the

utility triage effectively counteract the infrastructure vulnerability.

Additional information on the types of disrupted devices enlightens how the heterogeneous recovery is coupled with the structure of the distribution grid. The prioritized large failures for the severe and extreme events consist of primarily (i.e., > 89%) open substation breakers, with the non-prioritized large failures as reclosers and fused discs (see Supplemental Fig. 3). Substation breakers, located at the main power sources (substations) of the existing distribution grid, have to be restored with priority to provide electricity downstream. Meanwhile, restoring the large failures requires identification and isolation of all failures downstream, for both repair and safety of customers¹⁷. The time needed for failure identification increases with the scale of severe failure events¹⁷. In contrast, the prolonged small failures correspond to transformers close to customer property and fused cutouts (see Supplemental Fig. 3 and Supplemental Table 3). This implies that recovery is a complex network problem, where restoration can be dependent across different types of failures, and thus require subsequent study.

Disparity deepened in recovery from severe and extreme events

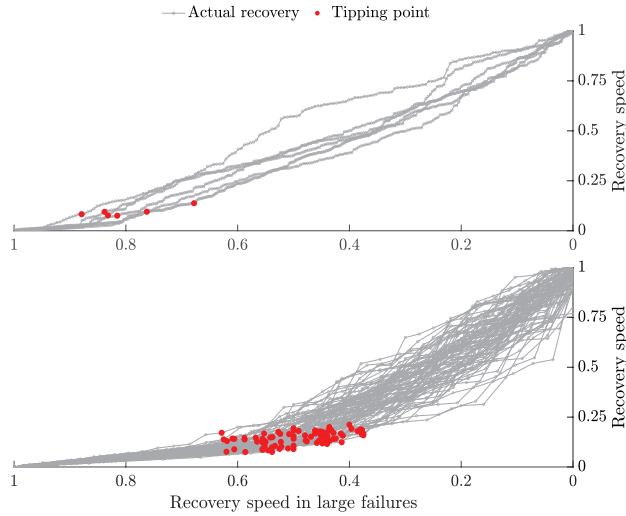
The disparity in recovery deepens when the failure events become severe or extreme. The heightened disparity is seen primarily by (a) a significant increased in large failures that cannot be prioritized, and (b) domination of small failures in dynamic evolution of delayed recovery.

The prioritized large failures consume less than 1% of the total downtime across the failure events of different severity. These prioritized large failures affected on average 1500 or more cus-

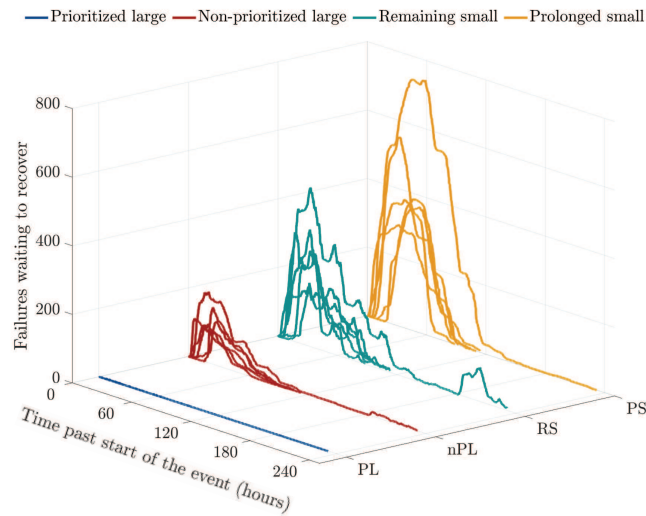
tomers, each of which recovered in less than 0.1 hours on average. However, such rapid recovery is difficult to sustain. The percentage of the customers affected by the prioritized large failures is reduced by 29% ~ 38% from the moderate events to severe and extreme disruptions as shown by the recovery scaling law (see Supplemental Fig. 2 and Supplemental Note 3). In other words, 29% ~ 38% more customers affected by large failures became non-prioritized shown in Fig. 2.

To gain further understanding of the non-prioritized large failures, we establish a baseline scenario as if all the large failures were prioritized for restoration (see Supplemental Note 4). The actual recovery speed of the large failures is then compared with the baseline. A tipping point emerges as shown in Fig. 3a, before which the failures recovered consistently fall in the prioritized large category (see Supplemental Fig. 5 and Supplemental Note 5). The average tipping point values shown in Fig. 3a reduce from 49% for moderate events down to 26% then 19% respectively for severe and extreme disruptions (Supplemental Note 5). Here, the 30% decrease in the level of prioritization of the large failures matches the 38% reduction of the rapidly recovered customers in the recovery scaling curves from the moderate to extreme disruptions in Fig. 2. Therefore, the disparity deepens in the recovery of the prioritized and non-prioritized failures when a disruptive event becomes severe or extreme.

Dynamic evolution of recovery from extreme events further shows vividly in Fig. 3(b), how the large and small failures recover differently throughout an entire disruption (Materials and methods, and Supplemental Fig. 8 for non-stationary failure-recovery processes). First of all, at a given time during a disruption, there were more prolonged small failures waiting for restoration



(a) Tipping points



(b) Temporal evolution of the four categories of failures

Figure 3: (a) Tipping points for extreme events (top) and moderate events (bottom). A tipping point corresponds to where the actual recovery speed of large failures starts to deviate from the baseline. Red circles show where the tipping point occurs and the gray curves correspond to the actual recovery for an event. For the moderate events, the population is plotted for the tipping points with values between 20-th and 80-th percentiles for better visualization. (b) Temporal evolution of the four categories of failures during the extreme events. The number of failures waiting to recover at a given time instance is plotted for the prioritized-large (blue), non-prioritized-large (red), remaining-small (green) and prolonged-small (yellow) failures. Each curve is for one of the six extreme events at the state of New York.

than any other categories. This shows that the prolonged small failures dominate delayed recovery. Next, the non-prioritized large failures that were pending for repair reach the maximum value about an average of 24 hours earlier than the prolonged small failures. Afterwards, the non-prioritized large failures enter the recovery stage (Materials and methods), and recover at a faster rate than the prolonged small failures. Comparing the worst impact at the peak, the maximum value is three times larger on average for the prolonged small failures than that of the non-prioritized large ones. In comparison, the prioritized large failures have the fewest pending repairs at any given time across all the extreme events. And, the the remaining small failures exhibit diverse variations. Therefore, small failures dominate delayed recovery during the extreme events.

How significant is the deepened disparity? The impact on customers provides an answer. First, the non-prioritized large failures result in the largest average customer interruption time (CMI - Customer Minute of Interruption) among the four failure categories. Importantly, the 30% increase of the non-prioritized failures results in 47 times more average CMI from the extreme disruptions than that of the moderate events (Supplemental Note 6). Next, our analysis finds that the growth rates of the actual cumulative customer downtime from the extreme events are drastically different for the four categories of failures (see Supplemental Fig. 6). The prolonged small failures stand out whose total downtime soars at a fastest rate, 3.5 ~ 5.7 times of that for the non-prioritized large failures. Furthermore, the prolonged small failures affected 60 ~ 800 customers for a moderate disruption but 3500 ~ 8700 users for an extreme event. The customers affected by the prolonged small failures regain power within 24 hours for the moderate events but experience interruptions as long as 170 hours for the severe and extreme disruptions. There is also 20% in-

crease of the smallest failures that affected one customer from the extreme disruptions compared with the moderate events (also observed by the Nor'easters in New Jersey 2018 ²⁵). About 48% (i.e., 1444) of those smallest failures in an extreme event are prolonged on average, representing the longest interruption time. This demonstrates that the extreme events induced particularly more failures close to customer properties, which are likely to experience delayed recovery. Overall, the impact is significant when the disparity deepens, reflected by the impact on customers from both large and small failures demonstrated across the service region at New York state in Fig.4.

Generalization to the state of Massachusetts

Can our analysis scale up to different service territories? Different service regions are known to have different grid structure and weather conditions ¹. However, minimizing the impact of failures on customers under constraints is a principle of recovery that guides restoration services in all regions by FEMA ¹⁷. Thus, it is important for us to explore the generalizability of our approaches to entirely different locations that are nevertheless under the same recovery guideline. We conduct a case study, focusing on the recovery from a major event, Super Storm Sandy, by the same service provider but in the state of Massachusetts.

The state of Massachusetts has fewer than 10 major storms from 2011 to February of 2019 at the service region in Massachusetts (see Supplemental Note 5). Super Storm Sandy in 2012 is one of the major storms that caused 4,011 failures and affected 330,298 customers for up to five days. Furthermore, the service region in Massachusetts is smaller (i.e., $\sim 3,870$ square miles) but more

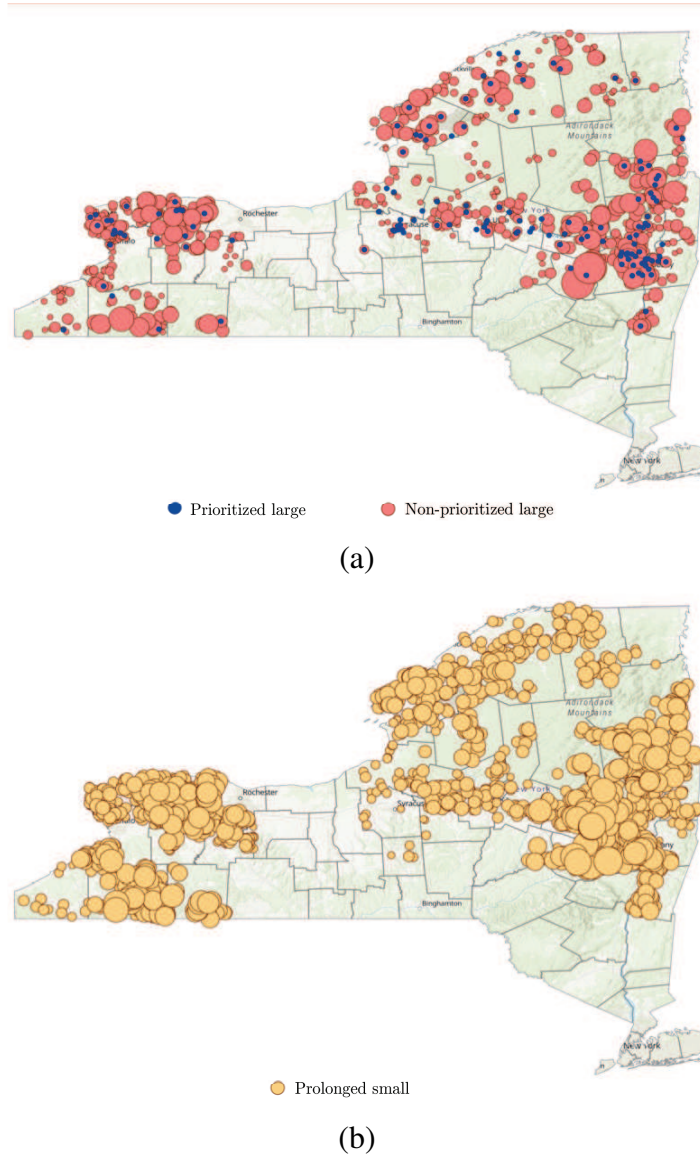


Figure 4: Geo-location of (a) large and (b) prolonged small failures in extreme events. The radius of the circles correspond to downtime durations from 0 to 150 hours. The blue markers in (a) correspond to the prioritized large failures. The red markers in (a) show the remaining large failures. The yellow markers in (b) represent the prolonged small failures in the extreme events.

densely populated than that at the state of New York.

We obtain the inference diagram (see Supplemental Fig. 5a) from the data at Massachusetts, where the clustered regions are identified using the same parameters as those in Supplemental

Note 2. The clusters do emerge for the prioritized-large and prolonged small failures, albeit the shapes of the clusters are different from those of New York State. We further obtain the recovery scaling law for this event in Supplemental Fig. 5b. Compared with that for New York State, the scaling curve has a similar shape and follows the similar $90 \sim 10$ rule. The prioritized-large and prolonged-small failures also exhibit the outstanding disparity in the percentage of affected customers and consumed downtime. The actual impact includes 338 large failures in total (and 35 prioritized large failures) that affected 42,554 customers with 39 hours aggregated downtime. As a comparison, the prolonged small failures are four times as many but correspond to $\frac{1}{5}$ fraction of the affected customers with 2,059 times longer total downtime hours. These results demonstrate both the promise for scaling up our analysis to other US states, and the need of incorporating differences in the grid structure and regional policies.

Discussions

This work performs a large scale field study on the recovery from large scale power failures using granular data from the operational distribution grid across a wide range of disruptions in two US states. Guided by unsupervised learning from non-stationary data, our analysis has drawn new and insightful knowledge on the recovery services governed by the commonly adopted government policy.

The restoration-service guided by the prioritized recovery policy is found to counteract the infrastructural vulnerability of the power distribution grid. Phenomenologically, the recovery prac-

tice, quantified by a novel recovery scaling law, prioritizes the restoration of the large failures so as to reinstall services for the majority of affected users. The resulting performance persists across the failure events of different severity, showing a desirable property of recovery.

The prioritized recovery, by design, does not optimize rapid restoration of all failures. In fact, heterogenous recovery heightened with the intensity of failure events for both large and small failures. There was a significant increase of the non-prioritized large failures that resulted in the largest total customer interruption time. This shows that the rapid restoration from prioritization does not sustain to severe and extreme failure events. Meanwhile, at any given instance during an extreme event, there were statistically more prolonged small failures waiting for repair than the large ones. Further, the prolonged small failures affected thousands of customers in an extreme event, each of whom experienced days of interruption. Hence, the impact of the disparity from severe and extreme events is significant. And, the depended disparity shows a fundamental limitation of the recovery under the prioritization policy.

Everyone who suffers from a natural disaster is important to the recovery services ¹⁹. A research question is how to overcome the fundamental limitation of the recovery. Our data analysis tells us that the restoration is constrained additionally by the structure of the distribution grid, where a certain large failures relating to the power components upstream have to be restored first ^{11,13}. Hence, a combined enhancement on the infrastructure ²⁹, recovery policy and disaster preparation is clearly a necessity, in order to reduce the interruption time to all users ^{6,30,31}. In this context, our study provides a benchmark for comparing an enhancement at the magnitude and scale of an

operational grid.

The data we use in this work are commonly available to most distribution grid operators in the US and parts of the world ^{9,11,14}. Thus, this study demonstrates that energy service providers have the ability to adopt data science ³²⁻³⁴, specifically, to turn their own data into knowledge, to benchmark and improve recovery. Further, such methodology adoption may offer profound impact to the community. Traditionally, a stigma runs deep that data-driven study on recovery may potentially reveal limitations of services. In fact, it is simply not a common practice for providers to study and share their own performance of service interruption using their own data. We hope that this study will encourage service providers and policy makers to take an active role in data analytics, to nurture a more collaborative environment.

Experimental procedures and methods

Unsupervised learning of recovery behavior from data: We derive a mathematical formulation for obtaining new knowledge on recovery services from the data. This is motivated by a formulation from Kearns et.al that evaluates the fairness of policies in machine learning ²¹. Here we view our study as evaluating the performance of recovery with the variables on failure characteristics and the restoration policy. The performance of recovery is not known. Neither is the relationship between the recovery performance and failure characteristics. Therefore, unsupervised learning is best suited for inferring new knowledge from the recovery behaviors and failure characteristics.

We let $X \in R^n$ represent failure characteristics where $n \geq 1$. The failure size is one such

characteristic, which is the number of customers affected by a failure. The type of disrupted devices is another failure characteristic, which includes substations as the primary energy sources at the distribution grid, and transformers close to customer property^{9,11}. Both the failure size and type of disrupted devices characterize the infrastructure of the distribution grid. $X \in A$ represents a set (A) of values for the variables (e.g., 100 or more affected customers, and damaged transformers at certain geographical coordinates). We let Y ($0 \leq Y \leq 1$) represent the recovery behavior on how fast a failure recovers, where Y is obtained by ranking the downtime duration from the shortest to the longest. Thus, $Y \in B$ represents the recovery speed, which is slow when $B : 0 \leq Y \leq y_1$, or rapid when $y_1 < Y < 1$. And, the boundary between the slow and rapid recovery is chosen as $y_1 = 0.5$ for simplicity. Other feature variables exist (e.g., weather and terrain conditions) that vary from event to event, and thus are considered as random factors. We let Y be a random variable characterizing the behaviors of recovery.

The recovery speed (Y) and failure characteristics (X) are random variables that in general are statistically dependent^{9,11,13}. The statistical dependence of (X, Y) is represented by their joint probability distribution $P(X \in A, Y \in B)$. For example, the strong dependence between the recovery speed and failure size reflects the impact of the utility triage on restoration. The independence of the recovery speed and failure characteristics provides a baseline ($P(X \in A)P(Y \in B)$). A metric ($f_{A,B}$) measures the degree of the dependence through a joint probability distribution relative to the baseline, where

$$f_{A,B} = P(X \in A, Y \in B) - P(X \in A)P(Y \in B). \quad (1)$$

The recovery speed and failure characteristics are positively dependent when the metric exceeds a threshold.

The unsupervised learning is implemented by first estimating the empirical joint probability $\tilde{P}(X \in A, Y \in B)$ using our data. Then the maximum coverage regions on (A, B) are obtained for $f_{A,B}$ to exceed a chosen threshold of 5% of the maximum value. And, such a condition is satisfied with a sufficiently small error bar $Err(f_{A,B})$. The error bars are obtained through 5-fold cross validation for each event and averaged between the training and test data across a given type of failure events (see Supplemental Note 2). The resulting coverage regions correspond to clusters in unsupervised learning²². Such an unsupervised learning algorithm is applied to the three types of the failure events from the moderate to severe and extreme (see Supplemental Note 2).

Non-stationary recovery of the four categories: Failure and recovery are modeled as non-stationary random processes in our prior work^{9,11}. The failures waiting to recover, referred to as pending repairs, represent the first-order interaction of failure and recovery processes^{11,35–37}. The maximum number of the pending repairs separates the failure-recovery processes into two stages, as illustrated by a typical example of an extreme failure event in Supplemental Fig. 8. While the failures can occur and recover at any time, the first stage is dominated primarily by the failure occurrences until the number of pending repairs reaches the maximum value. The second stage

is dominated by the recovery process, where recovery rate exceeds the failure rate, reducing the number of pending repairs from the peak. The slope for the number of pending failures to decrease from the peak value illustrates the rapidity of restoration.

Such non-stationary properties are extended directly to include the four categories, showing the dynamic evolution of delayed recovery. Let $R(t|c_i)$ be either the number of failures (or affected customers) in Category c_i ($1 \leq i \leq 4$), waiting to recover at time t . Then

$$R(t|c_i) = E\left\{\int_0^t G(t, v|c_i)dv\right\}, \quad (2)$$

where $G(t, v|c_i)$ is either a failure or customer affected in Category c_i , $1 \leq i \leq 4$, that occurs at time v but yet to recover at time t , $0 < v < t$. The integration adds up over all such failures or affected customers occurred in $[v, t]$. The expectation E is over randomly occurring failures or affected customers^{9,11}. $R(t|c_i)$ is estimated from the data on the four categories of failures (or affected customers) waiting to recover.

Data and temporal processing: The non-stationary property is also used for selecting a subset of the data samples for reliable analysis. Two sets of data are collected by this work. One is the primary data set for learning and analyzing restoration behaviors governed by a commonly-used prioritization policy on recovery. Such a data set is collected from a service region in the state of New York. The other is for extending analytics to the state of Massachusetts, particularly on the impact of different policies for declaring major failures events across state borders. We use the same variables for both data sets, and thus focus on describing the details of the primary data.

The main data set is obtained from a service region of 25,013 square miles at the state of New York. The data set includes 135,999 failures collected by a distribution system operator (DSO) from 2011 through January 2019. Total 33,497,547 customers were affected, with customer downtime duration of 778,718 hours (see Supplemental Table 2).

Each data sample contains detailed information regarding failures and recoveries: failure occurrence and recovery time in minutes, the number of affected customers per failure, the device type, geo- and grid-location of the disrupted components. Here a failure is represented by a damaged power component such as a transformer, or an activated protected device from an open substation breaker to a blown fuse. The grid locations of failures are highly coupled with the device types^{9,11} and thus not used in this work. Geo-locations are used mostly for visualization.

This work focuses on the available data to distribution system operators where failures were reported by customers. As such, some of the small failures might not be reported on time until discovered later. Some other outages, particularly those during recovery process, may be induced by restoration itself that had to turn off the electricity supply for repair. Thus, we extract reliable data for our study based on the non-stationary random processes discussed above¹¹. To be specific, most failures with long durations occurred at the first stage when restoration was overwhelmed by rapidly occurring failures. Hence, the maximum number of pending repairs is an indicator for separating data samples into the two stages for severe failure events (see Supplemental Note 7).

A total of 66% of failures in extreme events occurred in Stage 1 while the remaining 34% at Stage 2. In particular, at the failure stage (i.e., Stage 1), there are 87% of large failures (each of

which affected 100 or more customers); 75% of small-size failures except for one customer failures (each of which affected 2 ~ 100 customers. For the failures where each affected one customer, 53% occurred in Stage 1 whereas the remaining were in Stage 2. Therefore, given the significantly larger impact, both in terms of the number of customers affected and interruption durations, we use failures that occurred at the failure stage of the extreme and severe disruptions for our analysis.

We note that the majority of the failures that occurred during the recovery stage has relatively short interruption durations. Some of those interruptions on electricity supplies were indeed planned outages for necessitating repairs. Hence, the failures occurred at the first stage represent the majority induced by exogenous weather events (consistent to the data we used in the prior work¹¹). Additionally, the failure data at Stage 1 are considered to be reasonably accurate in interruption durations, since certain small failures were found during the recovery stage which might have occurred earlier (this of course can also occur to the small failures at Stage 1 to a lesser degree). Therefore, we use the data from the failure stage (Stage 1) in our analysis. Overall, using the data from Stage 1 provides conservative estimates of recovery behavior, since our data preprocessing extracts failures that were naturally initiated by an exogenous event (consistent to the data we used in the prior work¹¹). Different from what used in our prior work¹¹, the data we leave out in Stage 2 exclude a minute portion of failures with short durations. As such, our results here are more conservative in estimating the impact of the small failures than the prior work¹¹. While this may introduce a minute difference in actual percentages of small failures, the findings are consistent through out our previous and current study: There were more (prolonged) small failures than the large ones, and those small failures affected a lot fewer customers but experienced much longer

downtime durations.

Limitations of data and methods: Data used by this work enable learning the behavior of recovery, which results in insights on the policies. However, additional data are needed on terrain conditions, topological characteristics of the grid, and detailed impact on customers. Such data will help identify causal relations beyond behavioral learning, which is needed for enhancing services and policies as well as infrastructure enhancement. Further, additional micro data are needed from more US states. This will allow us to scale up our analysis and insights to more service territories.

1. The National Academies of Sciences, Engineering, and Medicine (U.S.) *Enhancing the resilience of the nation's electricity system*. Washington, DC: The National Academies Press. <https://doi.org/10.17226/24836> (2017).
2. Marsooli, R., Lin, N., Emanuel, K. et al. Climate change exacerbates hurricane flood hazards along US Atlantic and Gulf Coasts in spatially varying patterns. *Nature Communication* 10, 3785 (2019). <https://doi.org/10.1038/s41467-019-11755-z>
3. National Academies of Sciences, Engineering, and Medicine (U.S.) *Communications, Cyber Resilience, and the Future of the U.S. Electric Power System: Proceedings of a Workshop*. Washington, DC: The National Academies Press. <https://doi.org/10.17226/25782> (2020).
4. Executive Office of the President. Economic benefits of increasing electric grid resilience to weather outages. President's Council of Economic Advisers and the U.S. Department of Energy's Office of Electricity Delivery and Energy Reliability, Washington, DC. *Technical Report* (2013).
5. Guikema, S. & Nateghi, R. Modeling power outage risk from natural hazards. *Oxford Research Encyclopedia of Natural Hazard Science*, (2018).
6. Larsen, P.H., Sanstad, A.H., LaCommare, K.H., & Eto, J.H. Frontiers in the Economics of Widespread, Long-Duration Power Interruptions: Proceedings from an Expert Workshop. *Frontiers in the Economics of Widespread, Long-Duration Power Interruptions* (2019).
7. Smith, A.M., Posfai, M., Rohden, M. et al. Competitive percolation strategies for network recovery. *Scientific Report*, **9**, 11843 (2019).

8. AL-Kanj, L., Powell, W. & Bouzaiene-Ayari, B. The Information-Collecting Vehicle Routing Problem: Stochastic Optimization for Emergency Storm Response. *Arxiv*, arXiv:1605.05711 (2016).
9. Ji, C., Wei, Y. & Poor, H.V. Resilience of Energy Infrastructure and Services: Modeling, Data Analytics, and Metrics. *Proceedings of the IEEE*, **105**, no. 7, 1354-1366 (2017).
10. Bloomberg, M.R. A Stronger, more resilient New York. (City of New York) *PlaNYC Report* (2013).
11. Ji, C., Wei, Y, Mei, H. et al. Large-scale data analysis of power grid resilience across multiple US service regions. *Nature Energy*, **1**, 16052, <http://www.nature.com/articles/nenergy201652> (2016).
12. Dobson, I. Electricity grid: When the lights go out. *Nature Energy*, **1**, 16059 (2016).
13. Wei, Y. *et al.* Learning geotemporal nonstationary failure and recovery of power distribution. *IEEE Transactions on Neural Networks and Learning Systems*, **25**, 229–240 (2014).
14. Dunn, L.N., et al. Exploratory analysis of high-resolution power interruption data reveals spatial and temporal heterogeneity in electric grid reliability. *Energy Policy*, **129**, 206-214, (2019).
15. Yuan, Y., Dehghanpour, K., Bu, F., & Wang, Z. Outage detection in partially observable distribution systems using smart meters and generative adversarial networks. *arXiv:1912.04992v1* (2019).

16. Meier, A.V., Culler, D., McEachern, A. & Arghandeh, R. Micro-synchrophasors for distribution systems. *IEEE PES Innovative Smart Grid Technologies Conference (ISGT)*, 1-5, (2014).
17. Power outage incident annex to the response and recovery federal interagency operational plans. Homeland Security, June (2017).
18. Edison Electric Institute Understanding the electric power industry's response and restoration process, October (2016).
19. Roman M.O. *et al.* Satellite-based assessment of electricity restoration efforts in Puerto Rico after Hurricane Maria. *PLoS ONE* 14(6): e0218883. <https://doi.org/10.1371/journal.pone.0218883> (2019).
20. 16 CRR-NY 97.1, Notice of interruptions of service. *Office compilation of codes, rules and regulations of the state of New York, Title 16. Department of Public Service, Chapter II, Electric Utilities, Subchapter A. Service, Part 97.* Thomson Reuters. (2020).
21. Kearns, M., Neel, S., Roth, A. & Wu Z.S. Preventing Fairness Gerrymandering: Auditing and Learning for Subgroup Fairness. *Proceedings of the 35th International Conference on Machine Learning*, PMLR 80:2564-2572 (2018).
22. Duda, R.O., Hart, P.E., & Stork, D.G. *Pattern Classification* 2nd Edition, Wiley-Interscience, USA, October (2000).
23. National Oceanic and Atmospheric Administration, National Centers for Environmental Information, <https://www.ncdc.noaa.gov/stormevents/>.

24. Clauset, A., Shalizi, C. R. & Newman, M. E. Power-law distributions in empirical data. *SIAM Rev.* 51, 661 – 703, (2009).
25. State of New Jersey. Staff Report and Recommendations on Utility Response and Restoration to Power Outages During the Winter Storms of March 2018. New Jersey Board of Public Utilities. *Technical Report* (2018).
26. IEEE Power & Energy Society. *IEEE Draft Guide for Electric Power Distribution Reliability Indices*. IEEE P1366/D6 1-40 (2011).
27. Warren, C. A. et al. Classification of Major Event Days. *IEEE Power Engineering Society General Meeting*, 466-471 (2003).
28. Zio, E. Challenges in the vulnerability and risk analysis of critical infrastructures, *Reliability Engineering & System Safety*, Elsevier, 152, 137-150 (2016).
29. Dey, A.K., Gel, Y.R. & Poor, H.V. What network motifs tell us about resilience and reliability of complex networks. *Proceedings of the National Academy of Sciences*. **39**, 19368-19373, <https://doi.org/10.1073/pnas.1819529116> (2019).
30. Kelley-Gorham, M.R., Hines, P. & Dobson, I. Using historical utility outage data to compute overall transmission grid resilience. *arXiv:1906.06811*, 2019 (2019).
31. Baik, S., Davis, A.L., Park, J.W., Sirinterlikci S. & Morgan M.G. Estimating what US residential customers are willing to pay for resilience to large electricity outages of long duration. *Nature Energy*, **5**, 250-258 <https://doi.org/10.1038/s41560-020-0581-1> (2020).

32. Donoho, D. 50 Years of Data Science. *Journal of Computational and Graphical Statistics*. 26:4, 745-766, <https://doi.org/10.1080/10618600.2017.1384734> (2017).
33. Blei, D.M., & Smyth, P. Science and data science. *Proceeding of National Academies*, **114** (33), 8689-8692 (2017).
34. Yu, B & Kumbier, K. Vertical data science. *Proceedings of the National Academy of Sciences*. 117:8, 3920-3929 (2020).
35. Gallager, R.G. Stochastic processes: theory for applications. *Cambridge University Press* (2014).
36. Hajek, B. Random processes for engineers. *Cambridge University Press* (2015).
37. Bertsimas, D. & Mourtzinou, G. Transient laws of non-stationary queueing systems and their applications. *Queueing Syst. Theory Appl.* **25**, 115–155 (1997).

Acknowledgements

The authors thank Yun Wei, Scott Ganz, Richard Simmon, Mark Davenport for helpful discussions, Ramachandra Sivakumar for providing ArcGIS for data visualization, Eric O. Hsieh and Byeolyi Han for helping with data processing. Partial support from Strategic Energy Institute at Georgia Tech is gratefully acknowledged.